RAA 2015 Vol. **15** No. **3**, 333–347 doi: 10.1088/1674–4527/15/3/004
http://www.raa-journal.org *http://www.iop.org/journals/raa*

Research in Astronomy and Astrophysics

Sensitivity function analysis of gravitational wave detection with single-laser and large-momentum-transfer atomic sensors *

Biao Tang[1,2], Bao-Cheng Zhang[1], Lin Zhou[1], Jin Wang[1] and Ming-Sheng Zhan[1]

[1] State Key Laboratory of Magnetic Resonances, and Atomic and Molecular Physics, Wuhan Institute of Physics and Mathematics, Chinese Academy of Sciences, Wuhan 430071, China; *zhangbc@wipm.ac.cn*

[2] University of Chinese Academy of Sciences, Beijing 100049, China

Received 2014 March 26; accepted 2014 June 29

Abstract Recently, a configuration using atomic interferometers (AIs) had been suggested for the detection of gravitational waves. A new AI with some additional laser pulses for implementing large momentum transfer was also put forward, in order to reduce the effect of shot noise and laser frequency noise. We use a sensitivity function to analyze all possible configurations of the new AI and to distinguish how many momenta are transferred in a specific configuration. By analyzing the new configuration, we further explore a detection scheme for gravitational waves, in particular, that ameliorates laser frequency noise. We find that the amelioration occurs in such a scheme, but novelly, in some cases, the frequency noise can be canceled completely by using a proper data processing method.

Key words: gravitational wave detection — atomic interferometer — laser frequency noise

1 INTRODUCTION

Since gravitational waves are predicted from the theory of General Relativity, a direct detection of gravitational waves has become an exciting frontier of experimental physics (Gair et al. 2013). The initial detection scheme relied on resonant bar detectors (Weber 1969), which would be mechanically disturbed by passing gravitational waves, and then some other detectors were proposed, which had one or more arms with the idea that the length of arms would be influenced by passing gravitational waves. For the latter, VIRGO (Accadia et al. 2010) and LIGO (Abbott et al. 2009a) are the most sensitive detectors in this class, which are a kind of interferometer that operates by the change in apparent distance between mirrors as gravitational waves pass. Many efforts have also been made to improve the frequency range and sensitivity for probing possible gravitational waves, e.g. Advanced LIGO (Harry & LIGO Scientific Collaboration 2010), and a large space-based laser interferometer-based gravitational wave detector named eLISA (Amaro-Seoane et al. 2012). Although there has not been any definite or direct evidence to show the existence of gravitational waves up to now, these efforts defined an upper limit on the stochastic gravitational-wave background that has a cosmological origin (Abbott et al. 2009b). Another direction in efforts to detect gravitational waves is related to the use of atomic coherence, and the conceptual design includes

* Supported by the National Natural Science Foundation of China.

two well-known examples: Matter-wave Interferometric Gravitational-wave Observatory (MIGO) (Chiao & Speliotopoulos 2004; Speliotopoulos & Chiao 2004) in which atoms in the form of a wave act in the same role as photons in LIGO, and Atomic Gravitational Wave Interferometric Sensor (AGIS) (Dimopoulos et al. 2008a), which works with a similar mechanism as LIGO but replacing the macroscopic mirrors with freely falling atoms. A recent paper (Roura et al. 2006) showed that the scheme based on MIGO would be no better than LIGO, which reduced the attention focused on MIGO to some extent. However, the improved scheme of AGIS is still in progress, which is closely related to this paper.

Maybe it appears usual to ask why one would want to use atomic interferometers as sensors for gravitational waves, instead of the mirror configuration in LIGO. The reason is that the use of freely falling atoms or atomic interferometers as local inertial sensors reduces the requirement for elaborate seismic isolation, which limits the sensitivity of LIGO in the Hz-band or lower frequencies, so AGIS has an advantage over LIGO by detecting gravitational waves between 0.01 and 100 Hz. However, in AGIS, the Raman process in atomic interferometers still induces an uncontrollable noise through laser phase fluctuations, which are also a dominant source of background noise in the detection of gravitational waves using LIGO. The reason for the existence of laser frequency noises in AGIS (Dimopoulos et al. 2008b) is the use of two laser beams in the interaction with atoms, in which the pulses from the control laser are common to both interferometers and the phase contributions from this laser would be canceled in the final differential phase shift, but the noise in the phase of the passive laser cannot be canceled completely. This leads to a recent suggestion (Yu & Tinto 2011) for gravitational wave detection using a structure that is similar to AGIS but replacing the local inertial sensors with single-laser atom interferometers. This approach overcomes the laser frequency noise existing in gravitational wave detection using LIGO but still inherits the advantages of AGIS for suppression of vibration noise.

However, the measurement of interferometry is also limited by shot noise which is related to the number of particles involved in the interference process. Thus following an optimistic assumption (Dimopoulos et al. 2008a) about the number of atoms when operating an atomic interferometer, shot noise is still larger in an atomic interferometer than in an optical interferometer. In particular, the typical number of photons impinging on a photodetector is much more than the number of atoms in an atomic interferometer. Thus besides developing a new technology to increase the number of atoms, one has to use the large momentum transfer (LMT) (Dimopoulos et al. 2008a; Müller et al. 2008) to compensate for the low number of atoms. Based on this background, a new method for gravitational wave detection with atomic sensors was recently suggested (Graham et al. 2013), which not only overcomes the laser frequency noise using single-laser atomic interferometers, but also achieves LMT by adding some laser pulses between the basic beam splitter and mirror pulses. However, the authors in Graham et al. (2013) only produced a prototypical implementation for the mechanism used by LMT, and did not make a detailed analysis of the possible configurations for the new interferometer. This forms the main purpose of this paper, that is to analyze the configurations of the new interferometer and the difference in momentum transfer that results from different configurations. On the other hand, we will also attempt to analyze the cancelation of laser frequency noises with a direct and explicit mathematical expression.

In order to analyze the structure of new atomic interferometers, we introduce the sensitivity function (Cheinet et al. 2008) to distinguish different momentum transfers for different structures and thus the complex calculation for the final total phase difference using the standard method of non-relativistic quantum mechanics can be avoided. Section 2 will give a brief introduction to the sensitivity function, in particular how it can be applied to sense the signal from a gravitational field. In Section 3, we analyze possible configurations for the new interferometers and find some interesting phenomena related to some configurations. In Section 4, we present the results of laser frequency noise cancelation with an analysis of the total laser phase difference. Finally, we summarize our conclusions in Section 5.

2 SENSITIVITY FUNCTION

In this section, we will revisit the sensitivity function, without loss of generality, in the time-domain atomic interferometer first proposed by Kasevich & Chu (1991). The interferometer consists of a beam splitter-mirror-beam splitter ($\frac{\pi}{2} - \pi - \frac{\pi}{2}$) optical pulse sequence, and its sensitivity is limited to a large extent by the phase noise derived from the lasers as well as residual vibrations. Similar to the work of Cheinet et al. (2008), our investigation of the sensitivity function here relies on the assumption of short laser pulses that can be modeled as pure plane waves.

In the interferometer we consider here, the output of the results is presented by the change in energy level for the population of atoms, e.g. the probability of finding an atom remaining in the ground state when leaving the interferometer is $P = \frac{1+\cos(\Delta\Phi)}{2}$ where $\Delta\Phi = \Delta\Phi_s + \Delta\Phi_n$ is the total phase difference (Dimopoulos et al. 2008b; Kasevich & Chu 1992; Storey & Cohen-Tannoudji 1994; Peters et al. 1997; Zhang et al. 2013) between the two paths of the interferometer, which is also the basis of the experimental observation. In a measurement of the local gravitational field of Earth, the leading order of the signal can be calculated as $\Delta\Phi_s = kgT^2$ where k is the effective wavevector describing the laser, T is the interrogation time between two sequential laser pulses, and g is the local gravitational acceleration. $\Delta\Phi_n$ is the interferometric phase from the interaction between three laser pulses and atoms, and it is usually locked to the value $\frac{\pi}{2}$ such that the transition probability is $\frac{1}{2}$, which ensures the highest sensitivity for any interferometric phase fluctuations. From the perspective of the configuration, the signal can also be regarded as being derived from a certain kind of interference, e.g. its influence is included in the interferometric phase $\Delta\Phi_n$. Thus it is not hard to understand why noises usually constrain the sensitivity of the interferometer. In the following, we will consider $\Delta\Phi = \Delta\Phi_n$ and $\Delta\Phi_s$ enters into the total phase difference as the influence of the gravitational field on the interferometric phase. In particular, we will consider the same interferometer but with a single laser pulse that interacts with the atom, and thus the Raman process is replaced with a single photon transition and the redundant effects related to the ac Stark shifts would disappear (Weiss et al. 1994; Peters et al. 2001). In this case, the signal, expressed by the leading order phase shift in a local gravitational field is proportional to the difference in atomic energy level, which will be seen later.

As first suggested by Dick (1987) and then investigated in detail by Cheinet et al. (2008), the sensitivity of a time-domain atomic interferometer can be characterized by the sensitivity function, which quantifies the influence of a relative laser phase shift $\delta\phi$ occurring at a time t during the interferometer sequence onto the transition probability $\delta P(\delta\phi, t)$; it is then defined by Dick (1987) as

$$g(t) = 2 \times \lim_{\delta\phi \to 0} \frac{\delta P(\delta\phi, t)}{\delta\phi}. \tag{1}$$

If the origin for time is chosen at the middle of the second Raman pulse, the sensitivity function $g(t)$ is an odd function. For the three pulses $\frac{\pi}{2} - \pi - \frac{\pi}{2}$ with durations respectively $\tau - 2\tau - \tau$, we choose the initial time $t_i = -T$ and the final time $t_f = T$ to derive the expression of the sensitivity function as

$$g(t) = \begin{cases} \sin[\Omega(T+t)], & -T \leqslant t < -T+\tau, \\ 1, & -T+\tau \leqslant t < -\tau, \\ -\sin\Omega t, & -\tau \leqslant t < \tau, \\ -1, & \tau \leqslant t < T-\tau, \\ -\sin\Omega(T-t), & T-\tau \leqslant t \leqslant T, \end{cases} \tag{2}$$

where Ω is the effective Rabi frequency and $g(t) = 0$ for $|t| > T$ due to the phase jump that occurs outside the interferometer. As seen in Figure 1, the sensitivity function $g(t)$ is indeed an odd function, so in the analysis of the next section, we will present a sensitivity function with only the part $t < 0$. Usually, the Fourier transform of the sensitivity function is required, since noises that are closely related to the analysis of the sensitivity of an interferometer can be expressed in terms of

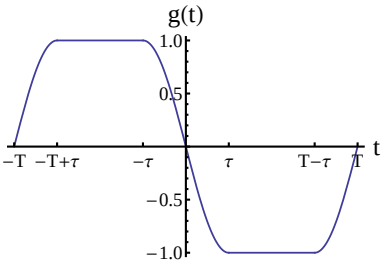

Fig. 1 The sensitivity function $g(t)$.

a power spectral density, which can be expanded in terms of frequency. Thus the transfer function, which is introduced in Appendix A is usually used in the analysis of the sensitivity, but in the present paper, we focus on the analysis of the structure of the interferometer, so the sensitivity function is enough. We will also use the transfer function when we discuss the advantages of some kinds of interferometers, e.g. the transfer of the influence of noises.

As shown by Cheinet et al. (2008), one can evaluate the fluctuations of the interferometric phase $\Delta\Phi$ caused by an arbitrary perturbation $\phi(t)$ by

$$\Delta\Phi = \int_{-\infty}^{+\infty} g(t) \frac{d\phi(t)}{dt} dt. \tag{3}$$

Of course, the influence due to the atomic acceleration will be sensed by the interferometer through the sensitivity function. In general, this type of time-domain atomic interferometer discussed here is an accelerometer. In the free evolution of the atom, its phase changes by $\phi_g(t) = \frac{\omega_a}{c} x = \frac{\omega_a}{c}(x_0 + v_0 t + \frac{1}{2} g t^2)$ where x_0 and v_0 are the initial position and velocity of the atom respectively. Then using Equation (3), we recover the signal of the interferometer

$$\Delta\Phi_s = \frac{\omega_a}{c} g T^2 + O(1), \tag{4}$$

where ω_a is the difference in atomic energy levels and $O(1)$ represents the terms related to τ or $\frac{1}{\Omega}$, which are negligible compared to the leading term. Here it is stressed that we ignore the negative sign before the leading order of $\Delta\Phi_s$ in this paper, without influencing our discussion. If the relativistic calculation is considered, like that by Dimopoulos et al. (2008b), and the corresponding geodesic is used to find the phase disturbance $\phi_g(t)$, more effects will be presented. Here the calculation is feasible, because the phase change of the atom induced by the gravitational field during the free evolution is equivalent to the phase change of the laser pulse by the fact that the gravitational field changes the positions of the interaction between the laser pulses and atoms. On the other hand, in the free evolution, the phase changes are actually $\phi_{g0}(t) = \frac{\omega_0}{c} x$ where ω_0 is the energy of the atomic ground state and $\phi_{g1}(t) = \frac{\omega_1}{c} x$ where ω_1 is the energy of the atomic excited state, but after the first beam splitter, the state of the atom is a superposition of the ground and excited states, so we only need to consider the change in the relative phase, $\phi_g(t) = \frac{\omega_a}{c} x$, where $\omega_a = \omega_1 - \omega_0$.

3 CONFIGURATION OF THE NEW ATOMIC INTERFEROMETER

In this section, we will use the sensitivity function to analyze the configuration suggested by Graham et al. (2013), which can be understood as a variant of a de Broglie wave interferometer that uses light pulses in the Mach-Zender configuration. This kind of atomic interferometer is derived from the time-domain atomic interferometer introduced in the last section, but with an obvious difference

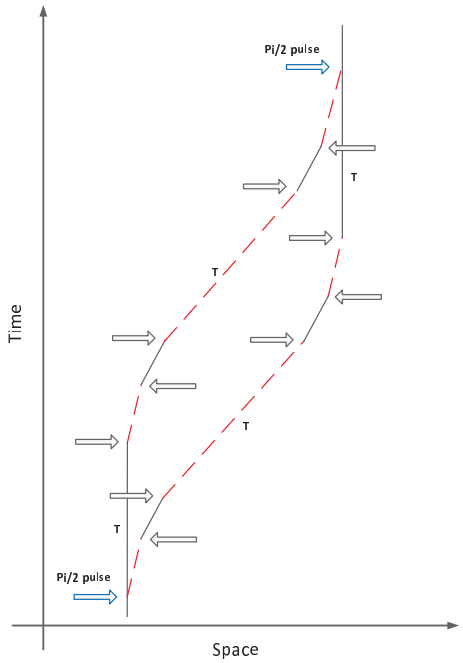

Fig. 2 A spacetime diagram of the proposed $N = 3$ configuration. The non-labeled arrows represent the π pulses, and the directions of the arrows are along the motion of the pulses. The points that are linked by the solid and dashed lines indicate the vertices at which the laser interacts with the atoms.

by adding some pulses between the basic beam splitters and the mirror pulse, which leads to an LMT. All added pulses are π pulses (to distinguish them from the basic mirror π pulse, we call these specific π pulses) which are designed to only interact with the required half the number of atoms, unlike the three basic pulses that interact with all atoms simultaneously but with different influences on each half. In order to implement the LMT, these specific π pulses must be arranged carefully. Here we will show that for a given number of specific π pulses, the momentum transfer will depend on *the sequence* (which includes a consideration of the direction of pulses and which halves of atoms will interact with the laser pulses) and *the time* (which means what time each pulse is applied). The case of $N = 3$ is used to show this. The sign N is slightly different from that used by Graham et al. (2013), and here our signs are related to the final leading order phase shift for the case with the largest momentum transfer; e.g. for the interferometer with $N = 3$ presented in Figure 2, it is $\sim 3\omega_a g T^2/c$. In particular, the case presented in figure 2 of Graham et al. (2013) has $N = 2$, according to our rule for signs.

It can be seen easily from the interferometer with $N = 3$ that there are four specific π pulses before the basic mirror pulse and the arrangement presented in Figure 2 is the case with the largest momentum transfer. Actually, there are many other ways to arrange the four π pulses, and the final phase shifts, to leading order, will include the possible results $\sim 2\omega_a g T^2/c$, $\omega_a g T^2/c$ and 0. There are 30 possible structures that we consider with different sequences and different times, but there is only one that can achieve the largest momentum transfer, i.e. the case of the final leading order phase shift is $3\omega_a g T^2/c$. It can be pointed out that the number of all possible configurations of interferometers is based on the assumption that the laser emitter is fixed in a given position or the basic beam splitters are oriented in the same direction. Then a problem arises: how can we know which is the LMT and how many momenta are transferred. One standard method is to calculate all

of the interactions that are included in the interferometry process to get the final leading phase shift, e.g. using the method of Dimopoulos et al. (2008b), when the effects of relativity are not required. Here we will provide another method that uses the sensitivity function. For the case $N = 3$ in Figure 2, due to the odd symmetry of the sensitivity function, we only write it for $t < 0$,

$$g_3(t) = \begin{cases} \sin\Omega(t+T)\,, & -T \leqslant t < -T+\tau\,, \\ 1\,, & -T+\tau \leqslant t < -T+3\tau\,, \\ \frac{1}{2}[3-\cos\Omega(T+t-3\tau)]\,, & -T+3\tau \leqslant t < -T+5\tau\,, \\ 2\,, & -T+5\tau \leqslant t < -T+7\tau\,, \\ \frac{1}{2}[5-\cos\Omega(T+t-7\tau)]\,, & -T+7\tau \leqslant t < -T+9\tau\,, \\ 3\,, & -T+9\tau \leqslant t < -9\tau\,, \\ \frac{1}{2}[5+\cos\Omega(t+9\tau)]\,, & -9\tau \leqslant t < -7\tau\,, \\ 2\,, & -7\tau \leqslant t < -5\tau\,, \\ \frac{1}{2}[3+\cos\Omega(t+5\tau)]\,, & -5\tau \leqslant t < -3\tau\,, \\ 1\,, & -3\tau \leqslant t < -\tau\,, \\ -\sin\Omega t\,, & -\tau \leqslant t < 0\,, \end{cases}$$

which is calculated in detail in Appendix B. Then for information about the gravitational field, to leading order we have

$$\Delta\Phi_s = \int_{-\infty}^{+\infty} g_3(t)\,\frac{d\phi_g(t)}{dt}dt = 3\frac{\omega_a}{c}gT^2, \tag{5}$$

and as expected, it includes the largest momentum transfer. This result is also seen implicitly from the sensitivity function itself, e.g. $g_3(t) = 3$ for $-T+9\tau \leqslant t < -9\tau$, as presented in Figure 3. However, the time that the specific π pulses are applied definitely reveals the desired information, that is the time for the eleven pulses calculated here is

$$\begin{aligned} t_1:\ &(-T) \to (-T+3\tau) \to (-T+7\tau) \to (-9\tau) \to (-5\tau) \to (-\tau) \to (3\tau) \to (7\tau) \\ &\to (T-9\tau) \to (T-5\tau) \to (T-\tau)\ . \end{aligned}$$

If we change the times but do not change the sequence, for example when taking

$$\begin{aligned} t_2:\ &(-T) \to (-T+3\tau) \to (-13\tau) \to (-9\tau) \to (-5\tau) \to (-\tau) \to (3\tau) \to (7\tau) \\ &\to (9\tau) \to (T-5\tau) \to (T-\tau)\,, \end{aligned}$$

we have $\Delta\Phi_s = 2\frac{\omega_a}{c}gT^2$ with the same integral as in Equation (5). Of course, we can also find the arrangement of the time for the sequence to make $\Delta\Phi_s = \frac{\omega_a}{c}gT^2$, but $\Delta\Phi_s = 0$ does not exist for the sequence. Thus, given the sequence shown Figure 2, there are five different arrangements of the times.

For a given time that the specific π pulses are applied, there are six different sequences in all for the case of $N = 3$. The schematics of the sensitivity functions of the other five sequences are presented in Figure 4. All 30 kinds of cases are summarized in Table 1. Some interesting cases exist, for example $\Delta\Phi_3 = 0$ and this configuration is impossible for the original interferometer consisting of a beam splitter-mirror-beam splitter ($\frac{\pi}{2} - \pi - \frac{\pi}{2}$) optical pulse sequence. More interestingly, for the sequence s6 and the time t1, $\Delta\Phi_3 = -\frac{\omega_a}{c}gT^2$, which includes a reversed momentum recoil.

When N increases, the kinds of possible interferometers will increase. For example, when $N = 4$, there are 140 kinds with 20 different sequences and seven different arrangements of times for each sequence. Notably, for every kind of interferometer, there is only one structure that achieves the largest momentum transfer, which is the final phase shift to leading order, $N\omega_a gT^2/c$.

It has to be pointed out that when the LMT interferometers amplify the signal, the noises are also simultaneously amplified, which attenuates the advantage of such interferometers. This can be easily seen from the white phase noise, and here we present a result from the vibration noises.

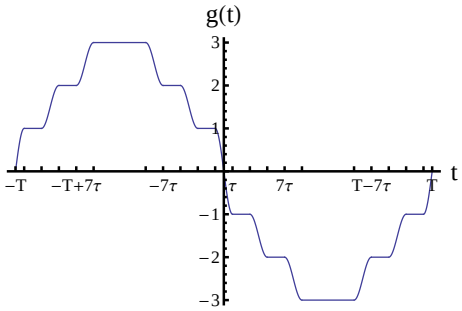

Fig. 3 The sensitivity function $g_3(t)$ for the case of $N = 3$ with the largest momentum transfer.

Table 1 The Final Leading Phase Shift ($\omega_a g T^2/c$) for the Structure with $N = 3$

Time/sequence	s_1	s_2	s_3	s_4	s_5	s_6
t_1	3	1	1	1	1	–1
t_2	2	2	0	2	0	0
t_3	2	2	2	0	0	0
t_4	1	1	1	1	1	1
t_5	1	1	1	1	1	1

Notes: The rows refer to different sequences, as presented in Figure 4. The columns refer to different times; t_1 and t_2 have been indicated in the paper;

t_3 : $(-T) \to (-T+3\tau) \to (-T+7\tau) \to (-T+11\tau) \to (-5\tau) \to (-\tau)$
$\to (3\tau) \to (T-13\tau) \to (T-9\tau) \to (T-5\tau) \to (T-\tau)$;

t_4 : $(-T) \to (-17\tau) \to (-13\tau) \to (-9\tau) \to (-5\tau) \to (-\tau) \to (3\tau) \to (7\tau)$
$\to (11\tau) \to (15\tau) \to (T-\tau)$;

t_5 : $(-T) \to (-T+3\tau) \to (-T+7\tau) \to (-T+11\tau) \to (-T+15\tau) \to (-\tau)$
$\to (T-17\tau) \to (T-13\tau) \to (T-9\tau) \to (T-5\tau) \to (T-\tau)$.

Figure 5 is a vibration spectrum measured in our lab. Assuming such a vibration happens in the measurement process of an interferometer, and we could estimate its influence on the final change in the population of atoms using Equation (A.6) in Appendix A, i.e. for the interferometer using three pulses described in the last section, the estimation of its influence is ~ 2.99 rad; for the interferometer with $N = 3$ described in this section, the estimation is ~ 11.8 rad. It can be easily seen that the influence from the vibration noise is amplified nearly four times compared to the previous one.

4 CONFIGURATION FOR GRAVITATIONAL WAVE DETECTION

Although the new interferometers with LMT amplify noises existing in the process of interferometry, many of the noises will be canceled when the two new interferometers are operated in a proper way, as in the case of the detection of gravitational waves (Yu & Tinto 2011). Compared with the above discussion, the influence of vibration noise is $\sim 2.9 \times 10^{-4}$ rad for the configuration with a baseline of $L = 1000$ km, which represents a very large suppression. See the schematic in Figure 6; the consideration is similar to the works of Yu & Tinto (2011) and Graham et al. (2013), with the atomic interferometers replaced by the new interferometers discussed in the last section. The laser emitter is laid at the left side and the secondary pulse is formed by the reflection from the mirror fixed at the right side. In particular, the time interval between the primary and secondary pulses depends on the distance between the mirror and the interferometer on the right.

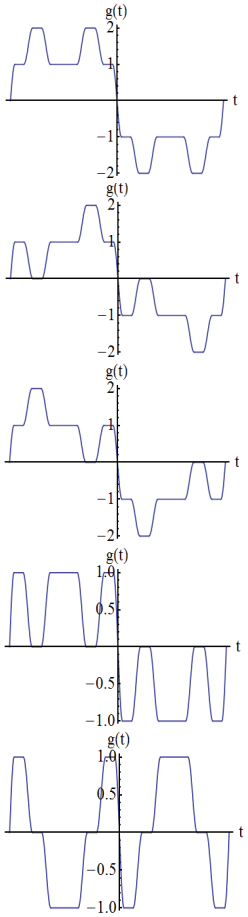

Fig. 4 The schematics of the sensitivity function for the interferometers with the other five sequences from s_2 to s_6 (following the order from top to bottom) but with the same time t_1, as listed in the first row of Table 1.

A related noise analysis had been made by Dimopoulos et al. (2008a) and Graham et al. (2013). In particular, Graham et al. (2013) pointed out a remarkable point that the configuration is immune to laser frequency noise for the detection scheme of gravitational waves that incorporates the new interferometers. Here we find some subtle differences, which will be discussed below, e.g. the suppression of the laser frequency noise is different between the cases of N being even or odd, for the case with the largest momentum transfer (in this section, we will only refer to the case with the largest momentum transfer, unless explicitly stated otherwise).

Firstly, we discuss the case for which N is even and assume that $N = 2$ without loss of generality. This case had been introduced in figure 2 of Graham et al. (2013) with a momentum transfer of $2\hbar k$, in which the phase change due to the interaction between the laser and the atom can be expressed as

$$\Phi_L = \phi_1 + \phi_2 - \phi_3 - 2\phi_4 - \phi_5 + \phi_6 + \phi_7,$$

where the subscripts are associated with the seven pulses in chronological sequence. Now we consider the phase change caused by the phase fluctuation $\phi(t)$ which is due to the laser instability (here

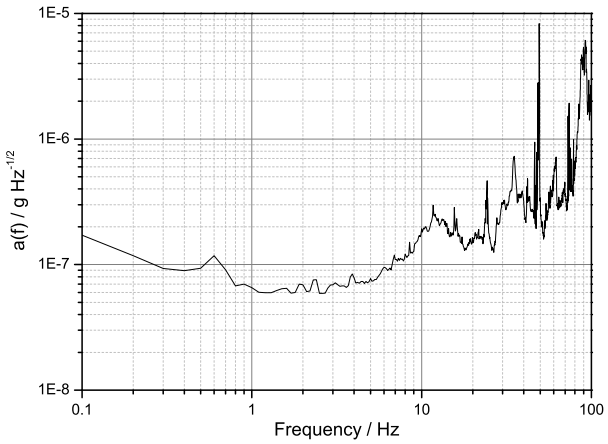

Fig. 5 The spectrum of the vibration measured in our lab using a seismometer, without any isolation system included in the measurement process. $a(f)$ is the acceleration noise power spectral density.

Fig. 6 A schematic of the detector used for gravitational waves that incorporates the new interferometers.

we ignore the other noise sources such as the fluctuation from atomic coherence), where t means the time that the pulse is emitted from the laser emitter since the phase of a laser does not evolve during its propagation in a vacuum. It is intuitive to use time delay interferometry (TDI) to cancel the laser frequency noise, which is also mentioned in the work of Graham et al. (2013), but we find this is not feasible for the present scheme. Similar to the method published by by Yu & Tinto (2011), the responses $R(t)$ of the new atomic interferometers to the laser phase noise can be written as

$$\begin{aligned} R_{21}(t) &= \phi(t) + \phi(t-3\tau-L) - \phi(t-T+5\tau) - 2\phi(t-T+\tau-L) \\ &\quad -\phi(t-T-3\tau) + \phi(t-2T+5\tau-L) + \phi(t-2T+\tau); \qquad (6) \\ R_{22}(t) &= \phi(t-L) + \phi(t-3\tau) - \phi(t-T+5\tau-L) - 2\phi(t-T+\tau) \\ &\quad -\phi(t-T-3\tau-L) + \phi(t-2T+5\tau) + \phi(t-2T+\tau-L), \qquad (7) \end{aligned}$$

where for brevity we take $c = 1$, t is chosen at the time that the final laser is emitted, "2" in the subscripts of $R_{21}(t)$ represents the case of $N = 2$ and "1" represents the left interferometer in Figure 6. In particular, the subscripts of ϕ are omitted, because the laser frequency noise is only caused by the laser emitter and is thus derived from the same function $\phi(t)$. If the laser is emitted from the left, the time of interaction between the laser and atoms in the right interferometer is delayed by $\Delta t = L$ and vice versa. By using the method of TDI, it can be expected that $\Delta R(t) = R_{21}(t-L) - R_{22}(t) = 0$, but actually this is not true for the case we are discussing, because a calculation gives $\Delta R(t) \neq 0$ by using expressions (6) and (7). This is because for the present scheme, not all the laser pulses are emitted in the same direction, which is different from the situation discussed by Yu & Tinto (2011). However, we find that, when τ is small enough compared with L and T (for example in a proposed

experiment by Graham et al. (2013), $\tau = 20$ μs, $L = 1000$ km which corresponds to 3 ms, and $T = 1.5$ s), the response functions can be written as

$$\begin{aligned} R_{21}(t) &= \phi(t) + \phi(t-L) - \phi(t-T) - 2\phi(t-T-L) \\ &\quad -\phi(t-T) + \phi(t-2T-L) + \phi(t-2T); \end{aligned} \tag{8}$$

$$\begin{aligned} R_{22}(t) &= \phi(t-L) + \phi(t) - \phi(t-T-L) - 2\phi(t-T) \\ &\quad -\phi(t-T-L) + \phi(t-2T) + \phi(t-2T-L). \end{aligned} \tag{9}$$

It is found that $\delta R(t) = R_{21}(t) - R_{22}(t) = 0$. So, one does not need to consider any time delay, since the laser frequency noise can be canceled at any time. Note that the cancelation is subtle, e.g. the first term in $R_{21}(t)$ is canceled by the second term in $R_{22}(t)$. This shows that the cancelation is better when the time interval is shorter (it is best if the time interval can be neglected like in the work of Graham et al. (2013) where the primary laser is triggered at time $t = 0$, and the secondary one at time $t = L/c$). This result can also be extended to any case for which N is even, since in that case, the number of laser pulses from one direction is equal to that from the other one.

However, we find the case for which N is odd is not the same. We show this by using the case of $N = 3$ presented in Figure 2, and its responses $R(t)$ of the new atomic interferometers to the laser phase noise can be expressed as

$$\begin{aligned} R_{31}(t) &= \phi(t) + \phi(t-3\tau-L) + \phi(t-7\tau) - \phi(t-T+9\tau) - \phi(t-T+5\tau-L) \\ &\quad -2\phi(t-T+\tau) - \phi(t-T-3\tau-L) - \phi(t-T-7\tau) + \phi(t-2T+9\tau) \\ &\quad +\phi(t-2T+5\tau-L) + \phi(t-2T+\tau); \end{aligned} \tag{10}$$

$$\begin{aligned} R_{32}(t) &= \phi(t-L) + \phi(t-3\tau) + \phi(t-7\tau-L) - \phi(t-T+9\tau-L) - \phi(t-T+5\tau) \\ &\quad -2\phi(t-T+\tau-L) - \phi(t-T-3\tau) - \phi(t-T-7\tau-L) + \phi(t-2T+9\tau-L) \\ &\quad +\phi(t-2T+5\tau) + \phi(t-2T+\tau-L). \end{aligned} \tag{11}$$

Again it is found that $\Delta R(t) = R_{31}(t-L) - R_{32}(t) \neq 0$ even though small τ is considered. In particular, it is also found that $\delta R(t) = R_{31}(t) - R_{32}(t) \neq 0$ when the time interval τ is neglected; this is seen as

$$\delta R(t) = \phi(t) - \phi(t-L) - 2(\phi(t-T) - \phi(t-T-L)) + \phi(t-2T) - \phi(t-2T-L).$$

As expected, $\delta R(t)$ is very small since $\phi(t)$ is a slowly varying function, which is required for any laser emitter. On the other hand, since $T \gg L$, we might have $\delta R(t) = 0$ by neglecting the time interval L. That is permitted if it is within the sensitivity of the interferometer. However, for the detection of gravitational waves, it is expected that the observable effect occurs in the time interval L, since the strength of the signal is proportional to the length L. It is found that the reason that laser frequency noise cannot be exactly canceled for any case with N being odd is due to asymmetry in the number of laser pulses from two directions. However, the laser frequency noise is suppressed to a large extent in the scheme with LMT.

Finally, we will point out the operational difference between $\Delta R(t)$ and $\delta R(t)$. $\Delta R(t)$ means that for each interaction, the pulse is the same for the first and the second interferometer. Such a situation is easy to understand from a physical perspective for the measurement of gravitational waves. In particular, it also achieves a large suppression of laser frequency noise in the present scheme. The reason that we use $\delta R(t)$ is that it leads to a complete cancelation of the laser frequency noise for the cases of even N. But for a single interaction, such operation means the pulses used to interact with the atoms are different for the first and second interferometers. Of course, this is only one choice for a data processing method, and we have to explain whether such operation can indicate the presence of gravitational waves. Fortunately, the latter operation will not change the signal since the response of the first interferometer to gravitational waves, $R_{\mathrm{GW}}(t)$, is usually regarded as zero (Yu & Tinto 2011). Thus $\delta R_{\mathrm{GW}}(t) = R_{1\mathrm{GW}}(t) - R_{2\mathrm{GW}}(t) = R_{1\mathrm{GW}}(t-L) - R_{2\mathrm{GW}}(t) = \Delta R_{\mathrm{GW}}(t)$.

5 CONCLUSIONS

In this paper we have investigated the sensitivity function and applied it to detection of the signal from the gravitational field of Earth through an atomic interferometer. We have also extended the application of the sensitivity function to a new atomic interferometer for which we have analyzed its configuration in detail. In our analysis, we found that given the number of laser pulses, there are some different methods needed to implement an LMT although the transferred momenta in each method are different. In particular, there is only one method that can achieve the largest momentum transfer (i.e. $N\hbar k$ momenta transfers for a scheme with the specific N defined in this paper); in all these methods, there are some configurations that give the results of zero momentum transfer and even inverse momentum transfer (e.g. the final leading phase shift is 0 or $-\frac{\omega_a}{c}gT^2$). For the configuration in Figure 6 used for the detection of gravitational waves, we have also analyzed how the laser frequency noise is canceled. We found that when N is even, the configuration is immune to the laser frequency noise with a proper data processing method; when N is odd, the configuration only gives a large suppression for the laser frequency noise. However, for the present situation that proposes a detection scheme for gravitational waves, the use of new atomic interferometers with LMT still represents good progress for the amelioration of the laser frequency noise.

Acknowledgements Financial support from the National Natural Science Foundation of China (Grant Nos. 11104324, 11374330 and 11227803) and the National Basic Research Program of China (973 program, 2010CB832805) is gratefully acknowledged.

Appendix A:

In this appendix, we will briefly introduce the transfer function.

In the paper, we use the sensitivity function to analyze the structure of an interferometer, but actually, maybe a little surprisingly, it can be noted that when we choose $t_i = -T-\tau$ and $t_f = T+\tau$, the expression for the sensitivity function becomes

$$g_c(t) = \begin{cases} \cos\Omega(T+t)\,, & -T-\tau \leqslant t < -T\,, \\ 1\,, & -T \ \leqslant t < -\tau\,, \\ -\sin\Omega t\,, & -\tau \leqslant t < \tau\,, \\ -1\,, & \tau \leqslant t < T\,, \\ -\cos\Omega(T-t)\,, & T \leqslant t \leqslant T\ +\tau\,. \end{cases} \tag{A.1}$$

Thus if the initial time or the final time is chosen by a change in τ, during that time, the sensitivity function will change from a sinusoidal to a cosinusoidal function. It is easy to understand why such a change is based on the assumption $\Omega\tau = \frac{\pi}{2}$. However, the transfer function is nearly the same for the two different choices, which is a mathematical representation of the relation between the input and output of a measurement system and is also usually called the weighting function.

For the interferometer we consider here, the Fourier transform of the sensitivity function is

$$G(\omega) = \int_{-\infty}^{+\infty} e^{-i\omega t} g(t)\, dt\,.$$

Using sensitivity functions (2), we have

$$G(\omega) = \frac{4i\Omega^2}{\Omega^2-\omega^2}\sin\left(\frac{\omega T}{2}\right)\left[\frac{1}{\Omega}\cos\left(\frac{\omega T}{2}\right)+\frac{1}{\omega}\sin\left(\frac{\omega\,(T-2\tau)}{2}\right)\right]. \tag{A.2}$$

In particular, for $\tau \ll T$, we have

$$G_c = \int_{-\infty}^{+\infty} e^{-i\omega t} g_c(t)\, dt\, (\omega) \simeq G(\omega)\ .$$

Thus although our paper analyzes the structure of the interferometers using the sensitivity function without discussing its dependence on the choice of the initial and final time, all results are applicable to any other analysis related to any change in the initial and final time.

Similarly, we can express the Fourier transform of the phase perturbation as

$$\Phi(\omega) = \int_{-\infty}^{+\infty} e^{-i\omega t} \phi(t)\, dt$$

and then put the reverse transform

$$\phi(t) = \int_{-\infty}^{+\infty} e^{i\omega t} \Phi(\omega)\, d\omega$$

into Equation (3). Thus we get

$$\Delta\Phi = -\int_{-\infty}^{+\infty} i\omega G(\omega)\, \Phi(\omega)\, d\omega\,. \tag{A.3}$$

Since the Fourier form $G(\omega)$ includes only a purely imaginary part as seen in Equation (A.2), the interferometric phase is also written as $\Delta\Phi = \int_{-\infty}^{+\infty} \omega\, |G(\omega)|\, \Phi(\omega)\, d\omega$. After the introduction of the transfer function

$$H(\omega) = \omega G(\omega)\ , \tag{A.4}$$

we have

$$\Delta\Phi = \int_{-\infty}^{+\infty} |H(\omega)|\, \Phi(\omega)\, d\omega, \tag{A.5}$$

which clearly demonstrates the process of how the interferometer responds to the phase disturbance (of course it also includes the signal). It is seen that if we put the Fourier transform of $\phi_g(t)$ into Equation (A.5), we can obtain the same result as Equation (4). A notable feature of the transfer function $H(\omega)$ is a low pass first order filtering, having an oscillating behavior with a periodic frequency of $\delta\omega = \frac{2\pi}{T}$ but less than the cutoff frequency $\omega_c = \frac{\sqrt{3}\Omega}{3}$ (Cheinet et al. 2008).

However, Equation (A.5) is not usually used because most studies have focused on the noise analysis but the power spectra of many noises are easier to describe, so the most popular one is the variance of the phase fluctuation,

$$\sigma_\Phi^2 = \int_0^{+\infty} |H(\omega)|^2\, S_\phi(\omega)\, d\omega\,, \tag{A.6}$$

where $S_\phi(\omega)$ is the power spectral density of the phase perturbation and is usually expressed as $S_\phi(\omega) = |\Phi(\omega)|^2$. It should be stressed that σ_Φ^2 is not directly related to the fluctuations of the interferometric phase, but are related to the average value of $\Delta\Phi$. In particular, the average is usually taken from a long sequence of measurement cycles at a fixed repetition rate which will lead to an aliasing phenomenon similar to the Dick effect (Dick 1987) in atomic clocks and increases the sensitivity of the interferometer at low frequencies.

An immediate examination is to use the white phase noise with no frequency dependence, $S_\phi(\omega) = S_\phi^0$. The result was given by Cheinet et al. (2008) and had a linear dependence on the inverse Raman pulse length. However, the pulse length will affect the number of participating atoms, which leads to shot noise and limits the sensitivity of the interferometer, so the optimum pulse length must be selected with reference to the experimental parameters.

Appendix B:

In this appendix, we will give a detailed calculation for the sensitivity function of the interferometer presented in Figure 2.

Considering the atom, which will go through the interferometer as a two-level system whose general state can be expressed as

$$|\varphi(t)\rangle = c_a(t)\,|a\rangle + c_b(t)\,|b\rangle$$

with

$$|c_a(t)|^2 + |c_b(t)|^2 = 1\,,$$

the evolution of the state under the interaction with the laser pulse is calculated with the change in the coefficients (Petelski 2005),

$$\begin{aligned} c_a(t_0+\tau) &= c_a(t_0)\cos\left(\frac{\Omega\tau}{2}\right) - ic_b(t_0)\,e^{i\phi}\sin\left(\frac{\Omega\tau}{2}\right), \\ c_b(t_0+\tau) &= c_b(t_0)\cos\left(\frac{\Omega\tau}{2}\right) - ic_a(t_0)\,e^{-i\phi}\sin\left(\frac{\Omega\tau}{2}\right), \end{aligned} \tag{B.1}$$

where Ω is the Rabi frequency, τ is the duration of the interaction and ϕ is the relative phase change during the interaction.

For the case of $N = 3$, there are 11 pulses, and in order to calculate the sensitivity function, besides the phase ϕ_0 carried by the pulses themselves which could be tuned during an experiment, a random phase change $\delta\phi$ during each interaction between the pulse and the atom may be introduced. For an illustration, we will calculate the result caused by the phase change $\delta\phi$ at time t during the first pulse, $-T < t < -T+\tau$, by splitting the pulse into two pulses of duration $T+t$ and $-T+\tau-t$. We start by assuming all atoms are in the state $|a\rangle$, and according to the sequence presented in Figure 2, the change in the coefficients after each pulse becomes,

$$\begin{aligned} c_{a1}(-T) &= 1\,, \\ c_{b2}(-T) &= 0\,; \\ c_{a1}(t) &= \cos\frac{\Omega(t+T)}{2}\,, \\ c_{b2}(t) &= -ie^{-i\phi_{01}}\sin\frac{\Omega(t+T)}{2}\,; \end{aligned}$$

$$\begin{aligned} c_{a1}(-T+\tau) &= c_{a1}(t-t-T+\tau) \\ &= c_{a1}(t)\cos\frac{\Omega(\tau-t-T)}{2} - e^{i(\delta\phi+\phi_{01})}c_{b2}(t)\sin\frac{\Omega(\tau-T-t)}{2} \\ &= \frac{\sqrt{2}}{2}(\cos^2\alpha + \sin\alpha\cos\alpha) - \frac{\sqrt{2}}{2}e^{i\delta\phi}(\sin\alpha\cos\alpha - \sin^2\alpha), \\ c_{b2}(-T+\tau) &= -\frac{\sqrt{2}}{2}ie^{-i\phi_{01}}(\sin^2\alpha + \sin\alpha\cos\alpha) - \frac{\sqrt{2}}{2}ie^{-i(\phi_{01}+\delta\phi)}(\cos^2\alpha - \sin\alpha\cos\alpha), \end{aligned}$$

where $\alpha = \frac{\Omega(t+T)}{2}$ and $\Omega\tau = \frac{\pi}{2}$ for the first pulse with the change by a random phase $\delta\phi$. The subscripts a and b represent the two energy levels and 1 and 2 represent the different paths. Since there is no new random phase introduced in the following ten pulses, the change in the coefficients

is easily calculated according to the evolution (B.1). For the final pulse, we obtain the expression of c_a as

$$\begin{aligned} c_a(T) &= \frac{\sqrt{2}}{2}c_{a2}(T-3\tau) - \frac{\sqrt{2}}{2}ie^{i(\phi_{11}+\delta\phi)}c_{b1}(T-3\tau) \\ &= -\frac{\sqrt{2}}{2}ie^{i(-\phi_{02}-\phi_{03}+\phi_{06}+\phi_{07}+\phi_{08}+\delta\phi)}c_b(-T+\tau) \\ &\quad -\frac{\sqrt{2}}{2}e^{i(\phi_{09}-\phi_{04}-\phi_{05}-\phi_{06}+\phi_{10}+\phi_{11})}c_a(-T+\tau) \\ &= -\frac{1}{2}e^{i(-i\phi_{01}-\phi_{02}-\phi_{03}+\phi_{06}+\phi_{07}+\phi_{08}+\delta\phi)}(\sin^2\alpha+\sin\alpha\cos\alpha) \\ &\quad -\frac{1}{2}e^{i(-i\phi_{01}-\phi_{02}-\phi_{03}+\phi_{06}+\phi_{07}+\phi_{08})}(\cos^2\alpha-\sin\alpha\cos\alpha) \\ &\quad -\frac{1}{2}e^{i(\phi_{09}-\phi_{04}-\phi_{05}-\phi_{06}+\phi_{10}+\phi_{11})}(\cos^2\alpha+\sin\alpha\cos\alpha) \\ &\quad +\frac{1}{2}e^{i(\phi_{09}-\phi_{04}-\phi_{05}-\phi_{06}+\phi_{10}+\phi_{11}+\delta\phi)}(\sin\alpha\cos\alpha-\sin^2\alpha). \end{aligned}$$

Define $\Phi = \phi_{01}+\phi_{02}+\phi_{03}-\phi_{04}-\phi_{05}-2\phi_{06}-\phi_{07}-\phi_{08}+\phi_{09}+\phi_{10}+\phi_{11} = \frac{\pi}{2}$, and we get the final probability of finding the atom still in state $|a\rangle$,

$$\begin{aligned} P_a &= |c_a(T)|^2 \\ &= \frac{1}{4}[2+\cos\Phi(1+\cos 4\alpha+2\cos\delta\phi\sin^2 2\alpha)+2\sin\Phi\sin 2\alpha\sin\delta\phi] \\ &= \frac{1}{2}(1+\sin\Omega(t+T)\sin\delta\phi). \end{aligned}$$

Thus according to the definition (1) of the sensitivity function, we have it in the time interval $-T < t < -T+\tau$ as

$$g(t) = \sin\Omega(t+T).$$

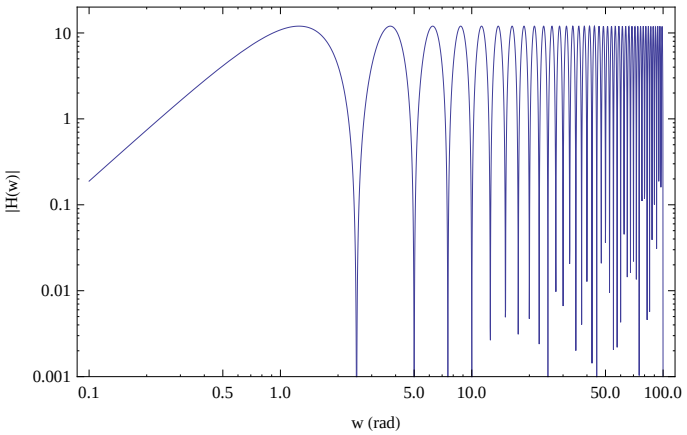

Fig. B.1 The transfer function H(w), which is the Fourier transform of the sensitivity function $g_3(t)$.

Then we can proceed in a similar way but the random phase change is introduced in the other ten pulses to obtain the sensitivity functions for those time intervals, and thus the whole sensitivity function $g_3(t)$ is acquired as presented in Section 3 of this paper.

The transfer function can be obtained using (A.4),

$$\begin{aligned} H(\omega) \;=\; & \frac{2\omega^2 i}{\Omega^2-\omega^2}\left[\frac{\Omega}{\omega}\sin\omega T-\cos\omega(T-\tau)+\cos\omega\tau\right]+2i\sin\omega\tau\Big[2\sin\omega(T-2\tau)\\ & +3\sin\omega(T-4\tau)+4\sin\omega(T-6\tau)+5\sin\omega(T-8\tau)+5\sin 8\omega\tau+4\sin 6\omega\tau\\ & +3\sin 4\omega\tau+2\sin 2\omega\tau\Big]+12i\sin\frac{\omega(T-18\tau)}{2}\sin\frac{\omega T}{2}\\ & +\frac{2\omega^2 i}{\Omega^2-\omega^2}\cos\omega\tau\Big[-\cos\omega(T-4\tau)-\cos\omega(T-8\tau)+\cos 8\omega\tau+\cos 4\omega\tau\Big], \end{aligned}$$

which is shown in Figure B.1.

References

Abbott, B. P., Abbott, R., Adhikari, R., et al. 2009a, Reports on Progress in Physics, 72, 076901

Abbott, B. P., Abbott, R., Acernese, F., et al. 2009b, Nature, 460, 990

Accadia, T., Acernese, F., Antonucci, F., et al. 2010, Journal of Physics Conference Series, 203, 012074

Amaro-Seoane, P., Aoudia, S., Babak, S., et al. 2012, Classical and Quantum Gravity, 29, 124016

Cheinet, P., Canuel, B., Pereira Dos Santos, F., et al. 2008, Instrumentation and Measurement, IEEE Transactions on, 57, 1141

Chiao, R. Y., & Speliotopoulos, A. D. 2004, Journal of Modern Optics, 51, 861

Dick, G. J. 1987, Local Oscillator Induced Instabilities in Trapped Ion Frequency Standards, in Proc. Nineteenth Annual Precise Time and Time Interval, 133

Dimopoulos, S., Graham, P. W., Hogan, J. M., Kasevich, M. A., & Rajendran, S. 2008a, Phys. Rev. D, 78, 122002

Dimopoulos, S., Graham, P. W., Hogan, J. M., & Kasevich, M. A. 2008b, Phys. Rev. D, 78, 042003

Gair, J. R., Vallisneri, M., Larson, S. L., & Baker, J. G. 2013, Living Reviews in Relativity, 16, 7

Graham, P. W., Hogan, J. M., Kasevich, M. A., & Rajendran, S. 2013, Physical Review Letters, 110, 171102

Harry, G. M., & LIGO Scientific Collaboration 2010, Classical and Quantum Gravity, 27, 084006

Kasevich, M., & Chu, S. 1991, Physical Review Letters, 67, 181

Kasevich, M., & Chu, S. 1992, Applied Physics B: Lasers and Optics, 54, 321

Müller, H., Chiow, S.-W., Long, Q., Herrmann, S., & Chu, S. 2008, Physical Review Letters, 100, 180405

Petelski, T. 2005, Atom Interferometers for Precision Gravity Measurements, Ph.D. Thesis, University of Firenze, Italy

Peters, A., Chung, K. Y., Young, B., Hensley, J., & Chu, S. 1997, Royal Society of London Philosophical Transactions Series A, 355, 2223

Peters, A., Chung, K. Y., & Chu, S. 2001, Metrologia, 38, 25

Roura, A., Brill, D. R., Hu, B. L., Misner, C. W., & Phillips, W. D. 2006, Phys. Rev. D, 73, 084018

Speliotopoulos, A. D., & Chiao, R. Y. 2004, Phys. Rev. D, 69, 084013

Storey, P., & Cohen-Tannoudji, C. 1994, Journal de Physique II, 4, 1999

Weber, J. 1969, Physical Review Letters, 22, 1320

Weiss, D. S., Young, B. C., & Chu, S. 1994, Applied Physics B: Lasers and Optics, 59, 217

Yu, N., & Tinto, M. 2011, General Relativity and Gravitation, 43, 1943

Zhang, B., Cai, Q.-Y., & Zhan, M.-S. 2013, European Physical Journal D, 67, 184